Advances in Science and Technology Research Journal

Advances in Science and Technology Research Journal, 2025, 19(10), 55–64
https://doi.org/10.12913/22998624/207748
ISSN 2299-8624, License CC-BY 4.0

Received: 2025.06.18
Accepted: 2025.08.15
Published: 2025.09.01

Mechanical properties of body centered cubic based lattice structures with varying aspect ratio in the loading direction

Kacper Rydzoń[1]

[1] Advanced Manufacturing Laboratory, Department of Manufacturing Systems, Faculty of Mechanical Engineering and Robotics, AGH University of Krakow, 30-059 Kracow, Poland
E-mail: krydzon@agh.edu.pl

ABSTRACT

Lattice structures have recently gained significant attention in research due to their excellent mechanical properties relative to their density and their high tunability through various design parameters. This study aims to investigate the effect of increasing the unit cell aspect ratio in the loading direction on the compressive properties of body-centered cubic (BCC)-based lattice structures. Compression tests were performed on both the base material and lattice structures with four different aspect ratios. In addition, tensile tests were conducted on the base material. The results show that Young's modulus, yield stress, and peak stress increase linearly with aspect ratio. Structures with higher aspect ratios are stiffer and can carry more load, but exhibit lower energy absorption. The findings confirm that a wide range of mechanical responses can be achieved. This study demonstrates that the aspect ratio can be effectively used as a design parameter for tuning mechanical properties while maintaining a constant relative density.

Keywords: mechanical properties, polylactic acid, lattice structures, body centered cubic, compressive loading, aspect ratio.

INTRODUCTION

Lattices, lattice materials or lattice structures are types of artificially designed spatial configurations that have gained a lot of interest in recent years due to their potential properties and features, which can be broadly altered by the right selection of design parameters, manufacturing technology and material [1–4]. As an example, they can be used as a core for sandwich panels, as an infill for lightweighting structural parts, or as a core for heat exchangers [5–7]. The possibility of achieving a wide spectrum of properties and the necessity of tailoring parts for specific applications enforces extensive analytical, numerical, and experimental research on lattices.

In general, the main design parameters that describe the geometry are relative density, unit cell type, unit cell dimensions, number of unit cells, thickness of the struts/walls and material [1]. Those may change depending on the design process or some may depend on each other, for example, the relative density and thickness of the struts [8]. Among the parameters mentioned, the relative density is the most significant, as highlighted by Ashby et al. [9]. The impact of relative density has been extensively investigated through both direct and indirect approaches and power laws models also called Gibson-Ashby models, predicting mechanical properties based on relative density have been introduced [1, 10–12].

In addition to relative density, the mechanical response of lattice structures and foams is largely determined by their deformation mode, which is typically classified as bending-dominated or stretch-dominated behavior [13, 14]. Bending dominated structures tend to be less stiff than structures dominated by stretch but offer better energy absorption [13]. In order to determine the type of deformation, the Maxwell equation or Gibson-Ashby model can be used [12]. Maxwell equation is based on analytical analysis of static

and kinematic relations in strut based structures and can be roughly used to determine the type of deformation. If structure is statically indeterminant, structure exhibits bending dominated behavior. In other cases, structure is stretch dominated.

Fabrication of lattice structures is limited by their complex geometry, which in most cases prevents the use of more established manufacturing techniques such as machining, moulding, casting, or forming. Although there are examples of using them for relatively simple lattices with limited complexity and dimensions, additive technologies are the main group of methods used for the fabrication of structures [1, 15–17]. The most widely used are fused filament fabrication (FFF) [18, 19], laser powder bed fusion - LPBF [20–22], and stereolithography (SLA) [10]. In the scope of this paper the most important is FFF technology, which will be used to prepare specimens. The main concerns which needed to be taken into account are the minimum feature size and the maximum overhang angle. Lattice structures, because of their complex geometries, tend to have features with an overhang angle greater than what most printers can offer. The potential solution to this issue is to design them via topology optimization with overhang constraints, which makes the lattice structure self-supporting [23, 24]. The other solution is to select optimal printing parameters that would enable error-free material deposition or at least minimize the risk of failure.

Geometry of the lattice structure can be modified in various ways which effect final properties. An interesting approach is to modify the aspect ratio of the cell or add features to existing filling types. Fadeel et al.[25] studied the effect of vertical strut arrangements in four different structures based on the body centered cubic (BCC) lattice structure. They find that the presence of vertical struts increases the strength of the lattice. Similar conclusions were brought up by Ye et al.[26] where they studied the influence of the addition of vertical struts to classic lattices. They confirmed that lattices with vertical struts exhibit higher stiffness and plateau stress than those without. Luo et al. [27] studied the anisotropy of elastic mechanical properties of triply periodic minimal surfaces (TPMS) lattice structures under different aspect ratios. Structures with increased aspect ratio in direction of loading can achieve great enhancement in terms of stiffness, peak stress and efficiency of energy absorption.

When comparing results from the previous references, it becomes evident that increasing the inclination angle of struts, up to the extreme case of vertical orientation, generally enhances the mechanical properties of lattice structures. In strut-based lattices, inclination angle is directly related to the aspect ratio of the unit cell. When the lattice type remains the same, increasing the aspect ratio in the loading direction alters the strut inclination accordingly. Surprisingly, few studies have focused directly on aspect ratio as a design parameter for BCC with most research focusing on TPMS structures [27].

Based on the above literature review, this study aims to address the identified gap by investigating how increasing the unit cell aspect ratio in the loading direction – while maintaining a constant relative density – affects the compressive mechanical properties of BCC-based lattice structures, a topic not previously explored by other researchers. To investigate this, compression tests were performed on various lattice configurations using digital image correlation (DIC). Additionally, to establish a baseline and better understand the relationship between material and lattice behavior, tensile and compression tests were conducted on the printed base material.

MATERIALS AND METHODS

Design of lattice structures

Lattice structures were created in Ntop [28] software by changing the aspect ratio of the BCC unit cell in the direction parallel to load. Aspect ratio is defined as follows:

$$AR = \frac{h}{w} \tag{1}$$

where: h is the height measured parallel to the load direction and w is the length of one of the edges perpendicular to the load direction.

The aspect ratio values were chosen so that the resultant number of cells in height is consecutive integers. This approach ensures that each unit cell within the lattice maintains uniform dimensions and remains fully defined. If alternative aspect ratio values were used, some unit cells would need to be cropped to fit within the design space, potentially influencing the mechanical behavior of the structure. Aspect ratio values cannot be

smaller than 1 because this would make manufacturing more difficult. The samples consisted of lattice part with dimensions of 50 × 50 × 50 mm and plates of 2 mm thick on top and bottom, total height of sample was 54 mm. An example of the resulting structure is shown in Figure 1a, where one of the complete lattices is displayed. Plates were added for an easier FFF fabrication process and a uniform load distribution during compression test. The relative density for each lattice was kept constant with a value of 20% so the thickness of the struts needed to be adjusted. Plates were not taken into account for the calculation of the relative density. Relative density was calculated according to equation:

$$\rho^* = \frac{\rho_l}{\rho} \tag{2}$$

where: ρ_l and ρ are, respectively, the lattice density and the base material density. For structures which are built from one material, relative density is equal to volume fraction.

In Figure 1b each created unit cell is presented. In nTop, the periodic lattice function was used to fill the designated volume with unit cells. A Boolean operation was then applied to merge the lattice with the top and bottom plates. In Table 1 design parameters used for lattices are presented.

Material and fabrication of specimen

Material which was used to fabricate specimen was polylactic acid (PLA) (Prusament PLA Prusa Galaxy black). The material was delivered in the form of a 1.75 mm filament. Specimens were fabricated using Prusa XL FFF printer with 0.4 mm nozzle. The printing parameters for every type of specimen were the same, some are provided in the Table 2. The main issue during specimen printing was features with angles grater then 45°. To address this problem, the speed of printing was reduced compared to the default PLA parameters provided by Prusa company.

Mechanical characterization

To study the compressive behavior of FFF-printed PLA, compression tests were performed on both the base material and the lattice structures using a Shimadzu AGX-V300 universal testing machine. To determine the mechanical properties of the material, samples were prepared according to the ASTM D695-15 standard, with a diameter of 12.7 mm, a height of 25.4 mm, and an infill density of 100%. Five of them were printed and tested to obtain statistically valid results. The crosshead speed was set at 1.3 mm/min and the test was carried out until a strain of 45% was reached.

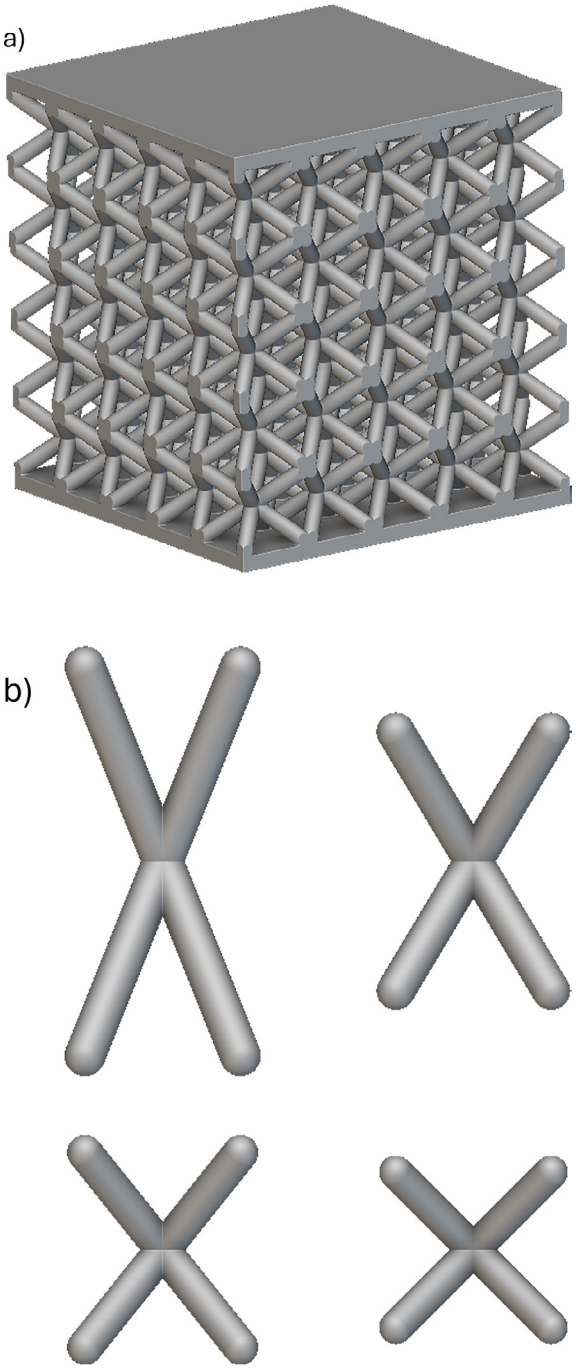

Figure 1. Designed lattice structures
a) example of lattice with AR = 1
b) studied unit cells, from top left
AR = 2.5, 1.67, 1.25, 1

Table 1. Design parameters for lattice structure

Id	Aspect ratio [-]	Number of cells in z [-]	Thickness [mm]
1	2.50	2	2.630
2	1.67	3	2.456
3	1.25	4	2.286
4	1	5	2.133

Table 2. Printing parameters

Parameter	Value
Perimeters printing speed [mm/s]	85
Infill printing speed [mm/s]	100
Layer height [mm]	0.2
Nozzle temperature [°C]	225
Heatbed temperature [°C]	60

The lattice structures were tested using the same setup, with the addition of a two dimensional DIC system and a crosshead speed of 2.6 mm/min. Three samples per type of lattice, 12 in total were compressed. A monochrome 16 MP camera was used to capture the images with 2.5 frames per second. Image postprocessing was performed using Alpha software, provided by XSight company. The complete experimental setup is shown in the Figure 2a. After testing, data from both the base material and lattice specimens were analyzed using MATLAB to determine Young's modulus, yield stress, peak stress, and energy absorption. Initial area to calculate stress was based on the surface area of lower plate. Initial height for strain calculation was taken as the height of the specimen (54 mm).

Tensile tests were conducted on the same machine as the compression tests, following the ASTM D638 standard with Type I specimen dimensions. Five specimens were printed in the flatwise orientation and tested. The infill pattern of the tensile samples was inclined at 45° to the loading direction and rotated 90° between successive layers. During the experiment, an extensometer with the gauge length of 50 mm was used to accurately measure strain for the calculation of Young's modulus and was retracted when the strain reached 0.035. The crosshead speed was set to 2 mm/min. Test data were analyzed using custom made

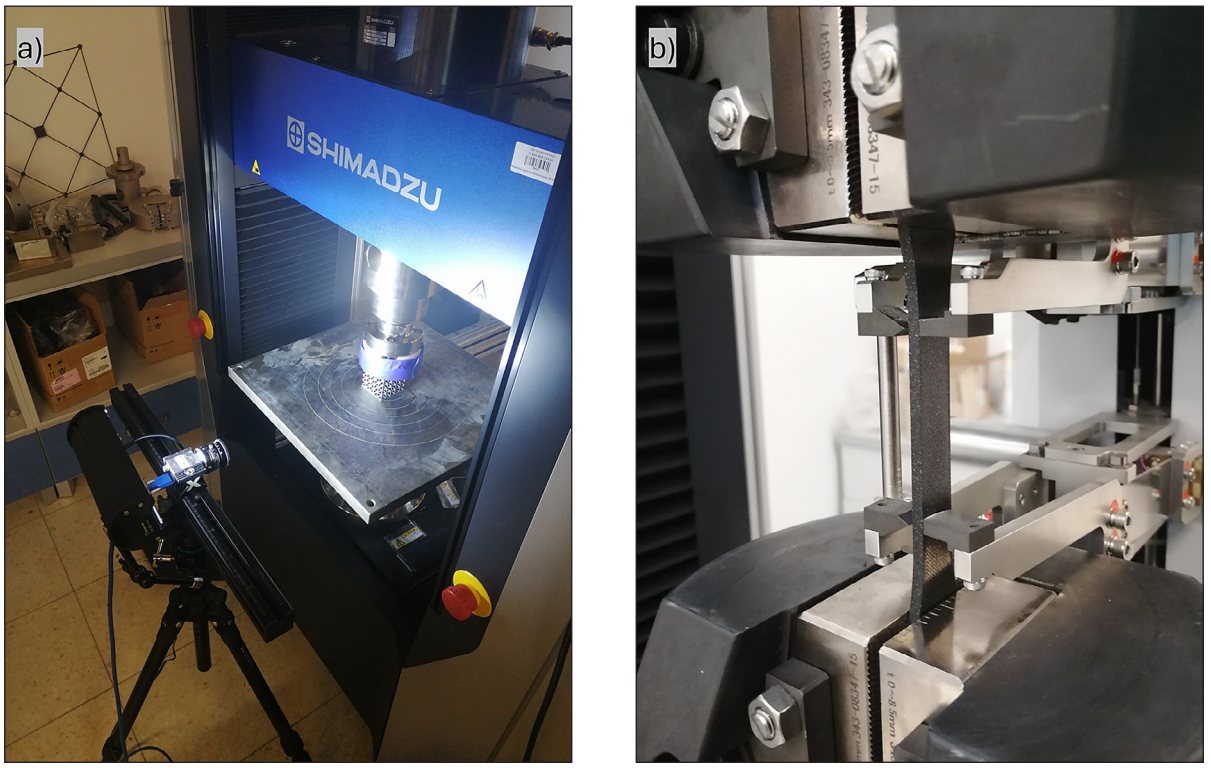

Figure 2. Experimental setup a) compression test, b) tensile test

MATLAB code. Young's modulus was calculated based on stress values between 2.5 MPa and 15 MPa. Yield stress was determined at 0.2% plastic strain, and energy absorption was computed as the area under the tensile curve up to the point of failure using MATLAB's trapz function. Experimental setup is shown in the Figure 2b.

RESULTS AND DISCUSSION

Mechanical properties of base material

Figure 3 presents the stress–strain plots for both the tensile and compression tests of the base material. The mechanical response is consistent across both tests, indicating high material and process stability. Table 3 shows the mechanical properties extracted from these curves. It is important to note that due to the strain rate dependent nature of PLA [29] and the anisotropy of FFF prints, accurately determining the exact mechanical properties of the load bearing material in the lattice structures is challenging. The base material tests provide a general reference point for evaluating the compressive behavior of the lattice structures but cannot be directly compared to them. This is primarily due to the complex geometry of the lattices, which leads to non-uniform deformation, complex stress states in struts and local variations in strain rate.

Mechanical properties of lattice structure

In Figure 4 the strain-stress response of each lattice structure is presented. Each curve consists of an elastic region and a plateau stress region, separated by a drop in stress. It can be observed that geometrical changes related to the aspect ratio have a significant influence on both regions. By increasing the aspect ratio, stiffness of the entire lattice structure also increases but also leads to a more sudden stress drop after achieving peak stress. This can be explained by the fact that the mechanism of the deformation is changing from bending dominated to stretch dominated. This can be further described using Figure 5. Force acting on the unit cell in downward direction is a vector consisting of two components, shear and normal. Shear force is causing bending in the strut while normal force is responsible for compression. Value of each component is determined by α angle following the Equation 3 and Equation 4. In analyzed case, when unit cells are extended in the direction of loading, the α angle decreases which increases share of normal force. Strut is stiffer for loads acting parallel to its axis than for bending. The result of this is a more rigid behavior of the unit cell which makes the whole lattice more resistant to deformation.

$$F_{shear} = F_{total} \cdot \sin\left(\frac{\alpha}{2}\right) \tag{3}$$

$$F_{normal} = F_{total} \cdot \cos\left(\frac{\alpha}{2}\right) \tag{4}$$

It is important to note that to maintain a constant relative density, the thickness of the struts must be increased. As a result, the cross-sectional area increases, effectively reducing stress and allowing the structure to carry more load without loss of geometric stability. Increasing the aspect ratio reduces the number of cells, which in turn

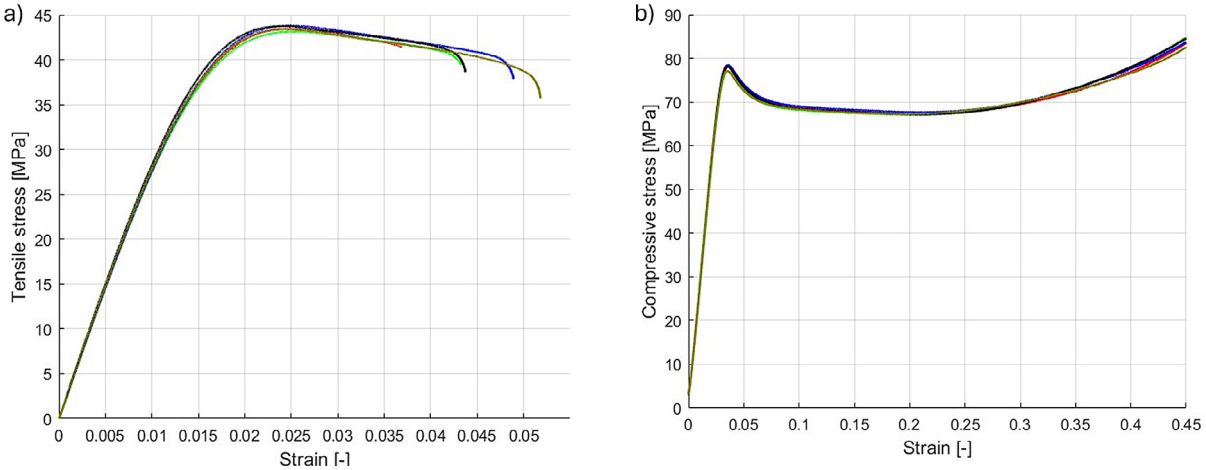

Figure 3. Experimental strain-stress curves of base material a) tensile, b) compression

Table 3. Base material tensile and compression mechanical properties

Test type	E ± std [GPa]	σ_y ± std [MPa]	σ_{peak} ± std [MPa]	Energy absorption [MJ/m^3]
Compression	2.73 ± 0.02	72.30 ± 0.52	77.79 ± 0.63	31.14 ± 0.10
Tensile	2.94 ± 0.04	36.41 ± 0.43	43.51 ± 0.28	1.56 ± 0.24

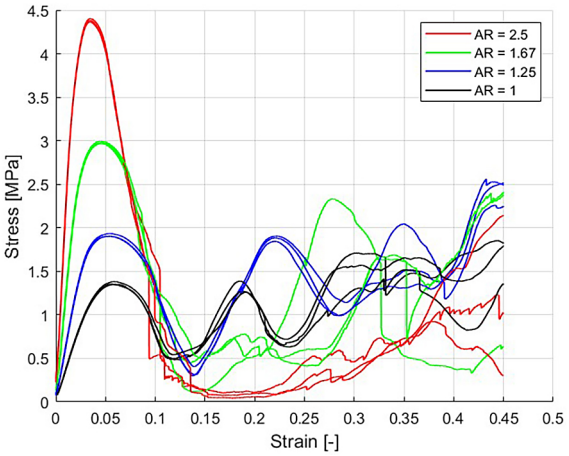

Figure 4. Experimental strain-stress curves of lattice structures

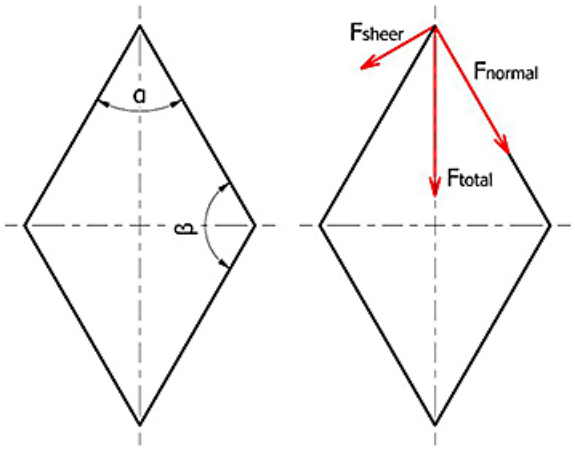

Figure 5. Angles and force in the unit cell

decreases the total number of struts in the structure. A smaller number of thicker struts leads to a greater accumulation of energy within each strut. This have impact on strut failure mechanism which is very complex. It is mainly influenced by the dominating force component and the properties of the anisotropic material. When the stress in a strut exceeds a critical threshold, it undergoes fracture between layers which are introduced by fabrication method, often leading to abrupt separation due to fast release of accumulated energy. For lattices with smaller aspect ratios, the strain required to reach the stress level that causes fracture is higher than for those with larger aspect ratios. This is clearly observed in the structures with aspect ratios of 2.5 and 1. In the former, sharp stress drops begin to occur at a strain of approximately 0.1, while in the latter, they occur around 0.3. Because of bending-dominated behavior, lattices with smaller AR are not able to carry high loads, but they do not lose their load carrying capability throughout the deformation of the specimen. After one layer experienced failure, others could carry the load, which can be seen as characteristic waves on the stress-strain curve.

Table 4 presents the experimentally obtained values of Young's modulus, yield stress, peak stress, and energy absorption for the tested lattice structures. Figure 6 shows the same mechanical properties which are plotted against aspect ratio together with error bars indicating ±3 standard deviations. For Young's modulus, yield stress, and peak stress, linear fit models were created and included in the plots. Due to its nonlinear nature, energy absorption is shown separately with individual data points, mean values, and ±3 standard deviation error bars.

The results indicate that the mechanical properties of the lattices scale approximately linearly with the aspect ratio. This trend can be attributed to the combined effect of the previously discussed mechanisms influencing the mechanical behavior of the structures. The high values of coefficients of determination (R^2 values close to 1) for all linear fits suggest that the lattice response during the initial stages of compression is highly reproducible. Based on these findings, it can be concluded that the aspect ratio is a suitable design parameter for tuning mechanical properties at a constant relative density particularly during initial stages of deformation.

Among measured parameters, energy absorption does not follow a linear trend and exhibits greater variability. This is because energy absorption is influenced not only by the load carrying capacity of the structure but also by its behavior during deformation. Failure in lattice structures is a stochastic process, when and how it occurs depends on various factors, including geometric

Table 4. Lattice structure compressive properties

AR [-]	E ± std [MPa]	σ ± std [MPa]	σ_{peak} ± std [MPa]	Energy absorption ± std [MJ/m^3]
1	36.78 ± 0.72	1.01 ± 0.01	1.36 ± 0.02	0.505 ± 0.046
1.25	63.38 ± 1.14	1.51 ± 0.03	1.91 ± 0.02	0.636 ± 0.011
1.67	121.59 ± 3.18	2.43 ± 0.04	2.98 ± 0.01	0.581 ± 0.051
2.5	224.33 ± 3.43	3.45 ± 0.04	4.38 ± 0.02	0.475 ± 0.051

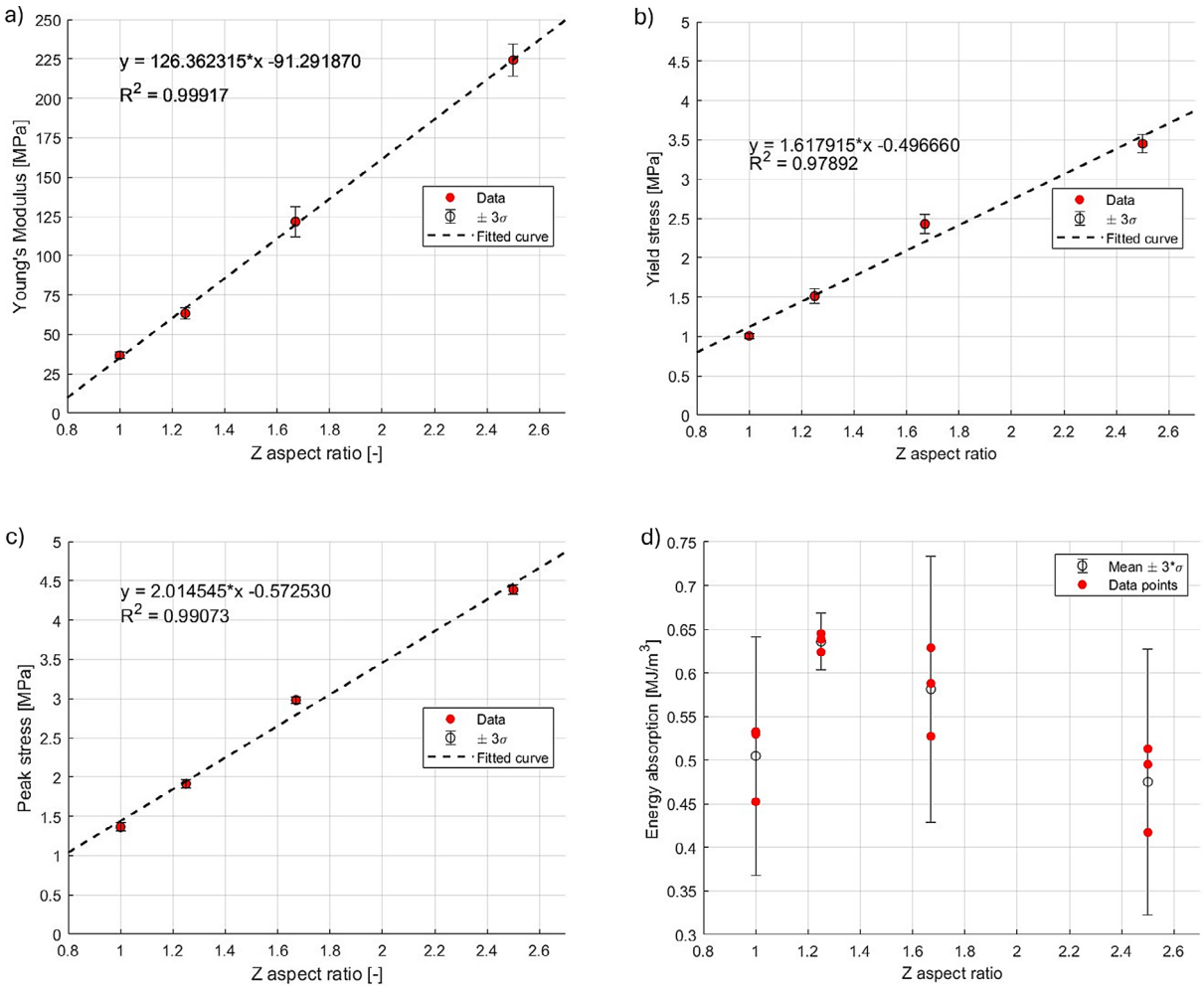

Figure 6. Mechanical properties of lattice structures relative to the aspect ratio a) Young's modulus, b) Yield stress, c) Peak stress, d) Energy absorption

imperfections and material defects to name a few. From the perspective of energy absorption, the lattice with an aspect ratio of 1.25 performs the best. It is capable of sustaining higher loads than the lattice with an aspect ratio of 1, while also maintaining structural integrity over a larger strain range compared to the AR 2.5 structure without experiencing a sudden loss of load bearing capacity.

Figure 7 presents post processed results from the digital image correlation analysis, showing the strain map (E1), values are only for comparison. In Figure 7b, a characteristic X-shaped strain pattern is visible, similar patterns are observed in forging processes of cylindrical billet. This region indicates where the initial localization of the strut failure will take place. Several struts undergoing bending can be observed, and in some cases, especially near the edges, layer separation occurs. Figure 7c shows the final stage of strut collapse within this same region. Struts outside of this area are still able to carry the load. Finally, Figure 7d illustrates the result of abrupt strut separation, energy accumulated in the strut is released, causing part of the lattice structure

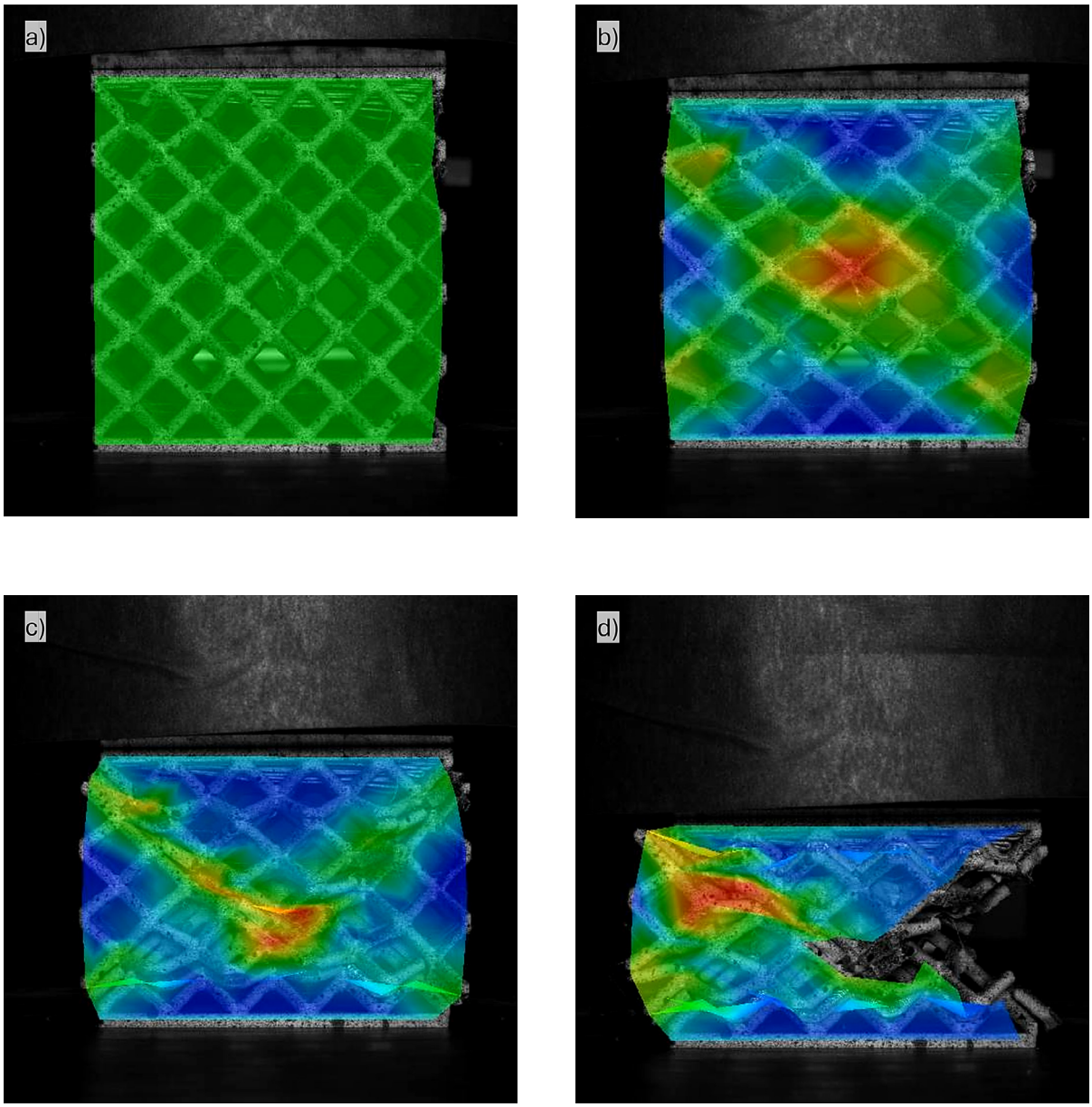

Figure 7. Digital image correlation, strain of lattice AR = 2.5 a) Initial state, b) characteristic strain localization, c) lattice after initial collapse, d) effect of sudden fracture

to be ejected. DIC results are shown only for the lattice structure for which AR is 1, as similar behavior was observed in other configurations, or they failed earlier, before reaching this collapse stage, as was the case for the lattice with an aspect ratio of 2.5.

The body centered cubic lattice structure is an example of a strut-based lattice, so it is likely that the results of this study are transferable to other lattices of the same type. However, without further research, it is difficult to conclude whether the AR is a universally relevant design parameter across all lattice geometries. Differences in node connectivity, spatial configuration, strut orientation, and strut thickness may cause the response to aspect ratio changes to deviate from linear trends observed in this study.

CONCLUSIONS

This study investigates the effect of varying the unit cell aspect ratio in the loading direction on the compressive mechanical properties of lattice structures. The main findings are as follows:

1. Mechanical properties can be significantly altered via changing the aspect ratio value. Higher values of AR results in higher stiffness

and strength. Changing the AR from 1 to 2.5 results in Young's modulus increase by a factor of 6.23, yield stress by 3.42, and peak stress by 3.22.

2. Aspect ratio can serve as a precise design parameter for tuning Young's modulus, yield stress, and peak stress of BCC based lattice structures at constant relative density. It was shown that these mechanical properties are changing linearly with AR.
3. Energy absorption does not exhibit a direct correlation with aspect ratio, as it depends on both the load bearing capacity and the deformation behavior of the lattice. When the aspect ratio is altered, these two factors are affected in opposing ways, an increase in one results in a decrease in the other. The highest energy absorption was observed in the lattice with an aspect ratio of 1.25, which represents a 25.9% increase compared to the lattice with an aspect ratio of 1.

REFERENCES

1. Khan N., Riccio A. A systematic review of design for additive manufacturing of aerospace lattice structures: Current trends and future directions. en. Progress in Aerospace Sciences 2024 Aug; 149:101021. https://doi.org/10.1016/j.paerosci.2024.101021
2. Liu R., Chen W., Zhao J. A review on factors affecting the mechanical properties of additively-manufactured lattice structures. Journal of Materials Engineering and Performance 2024 May; 33:4685–711. https://doi.org/10.1007/s11665-023-08423-1
3. Cuan-Urquizo E., Guerra Silva R. Fused filament fabrication of cellular, lattice and porous mechanical metamaterials: A review. Virtual and Physical Prototyping 2023 Dec; 18:e2224300. https://doi.org/10.1080/17452759.2023.2224300
4. Wu Y., Fang J., Wu C., Li C., Sun G., Li Q. Additively manufactured materials and structures: a state-of-the-art review on their mechanical characteristics and energy absorption. International Journal of Mechanical Sciences 2023 May; 246:108102. https://doi.org/10.1016/j.ijmecsci.2023.108102
5. Meng L., Qiu X., Gao T., Li Z., Zhang W. An inverse approach to the accurate modelling of 3d-printed sandwich panels with lattice core using beams of variable cross-section. Composite Structures 2020 Sep; 247:112363. https://doi.org/10.1016/j.compstruct.2020.112363
6. Oh SH., An CH., Seo B., Kim J., Park CY., Park K. Functional morphology change of TPMS structures for design and additive manufacturing of compact heat exchangers. Additive Manufacturing 2023 Aug; 76:103778. https://doi.org/10.1016/j.addma.2023.103778
7. NASA – Lightweighting Spacecraft with Latticing. Available from: https://www.ntop.com/resources/case-studies/replacing-spacecraft-supermaterial-with-high-performance-lattice/ [Accessed on: 2025 Apr 29]
8. Fan X., Tang Q., Feng Q., Ma S., Song J., Jin M., Guo F., Jin P. Design, mechanical properties and energy absorption capability of graded-thickness triply periodic minimal surface structures fabricated by selective laser melting. International Journal of Mechanical Sciences 2021 Aug; 204:106586. https://doi.org/10.1016/j.ijmecsci.2021.106586
9. Ashby M. F., Medalist R. F. M. The mechanical properties of cellular solids. Metallurgical Transactions A 1983 Sep; 14:1755–69. https://doi.org/10.1007/BF02645546
10. Guo P., Wu Y., Chen R., Lu B., Jia Y., Zhang W., Cao B., Yu S., Wei J. Development of strong, stiff and lightweight compression-resistant mechanical metamaterials by refilling tetrahedral wireframes. Virtual and Physical Prototyping 2024 Dec; 19:e2365852. https://doi.org/10.1080/17452759.2024.2365852
11. Xu S., Shen J., Zhou S., Huang X., Xie Y. M. Design of lattice structures with controlled anisotropy. Materials & Design 2016 Mar; 93:443–7. https://doi.org/10.1016/j.matdes.2016.01.007
12. Maconachie T., Leary M., Lozanovski B., Zhang X., Qian M., Faruque O., Brandt M. SLM lattice structures: properties, performance, applications and challenges. Materials & Design 2019 Dec; 183:108137. https://doi.org/10.1016/j.matdes.2019.108137
13. Ashby M. The properties of foams and lattices. Philosophical Transactions of the Royal Society A: Mathematical, Physical and Engineering Sciences 2006 Jan; 364:15–30. https://doi.org/10.1098/rsta.2005.1678
14. V Deshpande V., Ashby M., Fleck N. Foam topology: bending versus stretching dominated architectures. Acta Materialia 2001 Apr; 49:1035–40. https://doi.org/10.1016/S1359-6454(00)00379-7
15. Queheillalt DT., Murty Y., Wadley HN. Mechanical properties of an extruded pyramidal lattice truss sandwich structure. Scripta Materialia 2008 Jan; 58:76–9. https://doi.org/10.1016/j.scriptamat.2007.08.041
16. Kooistra G. Compressive behavior of age hardenable tetrahedral lattice truss structures made from aluminium. Acta Materialia 2004 Aug; 52:4229–37. https://doi.org/10.1016/j.actamat.2004.05.039
17. Feng LJ., Xiong J., Yang LH., Yu G. C., Yang W., Wu LZ. Shear and bending performance of new type enhanced lattice truss structures. International Journal of Mechanical Sciences 2017 Dec; 134:589–98. https://doi.org/10.1016/j.ijmecsci.2017.10.045

18. Sun Z., Guo Y., Shim V. Static and dynamic crushing of polymeric lattices fabricated by fused deposition modelling and selective laser sintering – an experimental investigation. International Journal of Impact Engineering 2022 Feb; 160:104059. https://doi.org/10.1016/j.ijimpeng.2021.104059
19. Daynes S. High stiffness topology optimised lattice structures with increased toughness by porosity constraints. Materials & Design 2023 Aug; 232:112183. https://doi.org/10.1016/j.matdes.2023.112183
20. Liu F., Zhou T., Zhang T., Xie H., Tang Y., Zhang P. Shell offset enhances mechanical and energy absorption properties of SLM-made lattices with controllable separated voids. Materials & Design 2022 May; 217:110630. https://doi.org/10.1016/j.matdes.2022.110630
21. Cobian L., Maire E., Adrien J., Freitas U., Fern´andez-Bl´azquez J., Moncl´us M., Segurado J. Effect of sample dimensions on the stiffness of PA12 lattice materials fabricated using powder bed fusion. Additive Manufacturing 2024 Aug; 93:104382. https://doi.org/10.1016/j.addma.2024.104382
22. Karmiris-Obratański P., Georgakopoulos-Soares I., Cichocki K., Lisiecka-Graca P., Papazoglou EL. Compressive and energy absorption properties of titanium hybrid lattice structures for bioimplant applications fabricated via LPBF. Materials & Design. 2025 Jun; 254:114045. https://doi.org/10.1016/j.matdes.2025.114045
23. Langelaar M. Topology optimization of 3D self-supporting structures for additive manufacturing. Additive Manufacturing 2016 Oct; 12:60–70. https://doi.org/10.1016/j.addma.2016.06.010
24. Zheng N., Zhai X., Jiang J., Chen F. Topology optimization of self-supporting structures for additive manufacturing via implicit B-spline representations. Computer Aided Design 2024 Oct; 175:103745. https://doi.org/10.1016/j.cad.2024.103745
25. Fadeel A., Mian A., Al Rifaie M., Srinivasan R. Effect of vertical strut arrangements on compression characteristics of 3d printed polymer lattice structures: experimental and computational study. Journal of Materials Engineering and Performance 2019 Feb; 28:709–16.https://doi.org/10.1007/s11665-018-3810-z
26. Ye J., Sun Z., Ding Y., Zheng Y., Zhou F. The deformation mechanism, energy absorption behavior and optimal design of vertical-reinforced lattices. Thin-Walled Structures 2023 Sep; 190:110988. https://doi.org/10.1016/j.tws.2023.110988
27. Luo Z., Tang Q., Ma S., Wu X., Feng Q., Setchi R., Li K., Zhao M. Effect of aspect ratio on mechanical anisotropy of lattice structures. International Journal of Mechanical Sciences 2024 May; 270:109111. https://doi.org/10.1016/j.ijmecsci.2024.109111
28. nTop, Release 5.14.3, nTop Inc., https://ntop.com
29. Balasubramanian M., Saravanan R., Shanmugam V. Impact of strain rate on mechanical properties of polylatic acid fabricated by fusion deposition modeling. Polymers for Advanced Technologies 2024 Mar; 35:e6335. https://doi.org/10.1002/pat.6335